Title

Coupled THM Modeling of Hydroshearing Stimulation in Tight Fractured Volcanic Rock

Journal

Transport in Porous Media, 108(1)

ISSN

0169-3913

Authors

Rinaldi, AP
Rutqvist, J
Sonnenthal, EL
et al.

Publication Date

2015-05-01

DOI

10.1007/s11242-014-0296-5

Peer reviewed

COUPLED THM MODELING OF HYDROSHEARING STIMULATION IN TIGHT FRACTURED VOLCANIC ROCK

A. P. Rinaldi[(a)], J. Rutqvist[(a)], E. L. Sonnenthal[(a)], T. T. Cladouhos[(b)]

(a) Lawrence Berkeley National Laboratory
1 Cyclotron Road
Berkeley, CA, 94720, USA
e-mail: aprinaldi@lbl.gov, jrutqvist@lbl.gov, elsonnenthal@lbl.gov

(b) AltaRock Energy
7900 E. Green Lake Drive N
Seattle, WA, 98115, USA
e-mail: tcladouhos@altarockenergy.com

submitted to Transport in Porous Media

ABSTRACT

In this study, we use the TOUGH-FLAC simulator for coupled thermo-hydro-mechanical (THM) modeling of well stimulation for an Enhanced Geothermal System (EGS) project. We analyze the potential for injection-induced fracturing and reactivation of natural fractures in a porous medium with associated permeability enhancement. Our analysis aims to understand how far the EGS reservoir may grow and how the *hydroshearing* effect depends upon system conditions. We analyze the enhanced reservoir, or hydrosheared zone, by studying the extent of the failure zone using an elasto-plastic model, and accounting for permeability changes as a function of the induced stresses. Results, for both fully saturated and unsaturated medium cases, demonstrate how the EGS reservoir growth depends on the initial fluid phase, and how the reservoir extent changes as a function of two critical parameters: the coefficient of friction and the permeability-enhancing factor. Moreover, whereas the stimulation is driven by the pressure exceeding a hydroshearing threshold, the modeling also demonstrates how the injection-induced cooling boosts the stimulation a bit farther.

INTRODUCTION

Thermo-hydro-mechanical (THM) analysis is essential when dealing with energy extraction from hot dry rock. The main concept of the Enhanced Geothermal System (EGS) is the exploitation of high thermal gradient regions through the creation (or reactivation) of a fracture network by increasing rock permeability, hence enhancing the circulation of water. EGS sites generally feature very low permeability formation (such as igneous rock in volcanic regions), where cold water is injected at moderate to high pressure to achieve *hydroshearing* (e.g., Cladouhos et al., 2009). Contrary to the more common hydrofracturing (or simply *fracking*) process, during hydroshearing reactivation, the injection pressure is kept below the minimum principal stress magnitude, causing existing fractures to dilate, slip and shear. Hydroshearing can permanently enhance permeability of natural fractures that conceptually should remain open because of self-propping of fractures due to surface roughness when the stimulation period ends and fluid pressure is reduced. As pointed out by Riahi and Damjanac (2013), the enhancement of the reservoir permeability during hydroshearing will depend on many *in situ* parameters, such as regional stress, geological, hydromechanical, and thermal parameters (e.g., frictional coefficient, intact rock permeability, heat capacity), as well as chemical processes associated with the injection of cold water.

The concept of *hydroshearing* is not new, but was first recognized and developed in the early 1980s, when Pine and Batchelor (1984) confirmed that the creation of new fractures was not the dominant process during the injection of water into the rock mass at great depth. Far more important was the shearing of natural joints and, in particular, those aligned with the principal stresses of the local stress field. In this concept, the joints fail in shear because the fluid injection reduces the normal stress across them and allows frictional slippage to occur before jacking, or creating of new hydraulic fractures. This was first demonstrated for the Cornwall hot dry rock project in the Carnmenellis granite where injection was conducted at depths greater than 2 km below ground level. Microseismic events detected during the high-flow rate stimulations indicated strike-slip shear consistent with the orientation of the natural joints and in-situ stress conditions. Meanwhile, in the field rock mechanics, the effects of fracture shear on permeability was studied through laboratory and in situ block experiments, with the first comprehensive study conducted at the Norwegian Getechnical Institude by Makurat et al., (1990). The concept of hydroshearing have since been employed at a number of EGS sites worldwide, including Hijoiro and Ogachi Japan as well as Soultz-sous-Forêts and Cooper Basin in Australia (Tester, 2006;

Ziagos et al., 2013). Experience gained in the last thirty years at EGS field projects has shown the critical importance of understanding and mapping the natural fracture system and the in situ stress field (Evans et al., 1999, Tester 2006). Trans-tensional environments (e.g., grabens) may be more amenable to successful manipulation than compressive stress regimes in EGS reservoir creation (Baria et al., 1999). Moreover, in the recent few years a number of EGS demonstration projects have been launched in the U.S., in which different variants of hydroshearing is employed in stimulation and permeability enhancement of the reservoir (Ziagos et al., 2013). These are funded by the U.S. Department of Energy's Geothermal Technology Program and include EGS demonstrations at Desert Peak and Brady’s Hot Springs, in Nevada, The Geysers in California, and finally the Newberry Volcano, Oregon (Ziagos et al. 2013). Three of these EGS demonstrations projects (Dessert Peak, Brady’s, and The Geysers) are located within or on the margins of existing hydrothermal fields, whereas one (Newberry Volcano), is located at an unexplored and undeveloped site (Ziagos et al. 2013).

In 2009, AltaRock Energy company was awarded a grant by the U.S. Geothermal Technology Program to plan and demonstrate an EGS at the Newberry Volcano, Oregon. During Phase I of the project, completed in April 2012, pre-stimulation field investigations were performed to understand the tectonic and volcanic setting, characterize the volume around the proposed EGS demonstration area, and plan the stimulation parameters. The stimulation plan was developed along the lines of Alta Rock Energy’s approach to hydroshearing in which the rock is stimulated in stages by injection in multiple isolated sections of the well bore using a injection pressure that is slightly lower than the pressure required for hydrofracturing, i.e. slightly lower than the minimum principal stress (Cladouhos et al., 2009).

A preliminary 3-D model of stress and fracture patterns was presented by Davatzes and Hickman (2011). Faulting is mainly evident along the caldera rim about 3 km from the designated injection well. There is no evidence of ring fractures or faults in the injection well (NWG 55-29) from drilling logs. Furthermore, Newberry Volcano has a very low seismicity rate (Cladouhos et al., 2013). An analysis of the natural fractures shows that there are two dominant sets that strike N-S and dip approximately 50˚ to the east and west (Davatzes and Hickman, 2011).

The stimulation took place between October and December 2012, during which three zones were created by injecting thermal-degrading zonal isolation materials (chemical diverters) to isolate already stimulated zones (Petty et al., 2013). Over 40,000 m^3 of water were injected in about 7 weeks of stimulation, reaching a maximum well-head pressure of about 16 MPa with over 200 induced microseismic events registered (Petty et al., 2013; Cladouhos et al., 2013). The maximum magnitude event (Mw = 2.39) was recorded during the period of highest well head pressure (P = 16.7 MPa). However, results show a strong correlation between the cumulative injected volume and cumulative logarithmic seismic moment, pressure does not correlate as strongly. The cloud of microearthquakes extends about 500–800 m from the injection well (Cladouhos et al., 2013).

A simultaneous analysis of flow rates, pressure, and seismicity that occurred at the Newberry EGS Demonstration site after the stimulation shows that the injectivity increased after reactivation, indicating an increase in permeability. The maximum well-head pressure (controlled at pump) resulted only after the injection of the chemical diverters, which reduced the flow rates. Moreover, no changes in pressure or flow rate seem to indicate the occurrence of hydrofracking or tensile failure, meaning that the pressure was below the minimum principal stress, but well within the range to achieve hydroshearing and its associated permeability enhancement.

Starting from the results obtained at Newberry Volcano, here we aim to study the hydroshearing effects during stimulation at an EGS site. We use as input the same stress field and rock properties (such as low permeability and porosity) measured at Newberry, and simulate the stimulation using a transient well-head pressure similar to the one recorded on the field. We do not aim to reproduce neither the seismicity nor the flow rate in exact detail, but aimed at a model that broadly represent the conditions and injection data at the Newberry. For example, we used a simplified but representative well pressure and a resulting flow rate that was similar to the measured one, though not matched in great detail.

The main goal of this work is to understand how hydroshearing may occur during stimulation, using the Alta Rock's hydroshearing approach (Claduohus et al., 2009). Through the use of the simulator TOUGH-FLAC (Rutqvist et al., 2002), we simulate a porous medium, which deforms when subjected to stress change. Fracture effect is simulated by assuming an anisotropic field of permeability, with the most of the fluid flow occurring then along the assumed fracture direction. Generally fracture aperture may change as subject to stress, and we simulate such a process by a permeability-stress relation. Furthermore, if the stresses reach a critical value, defined by the Mohr-Coulomb criterion, shear failure will occur, and the permeability of the porous medium will be further enhanced by a certain factor (generally between 2 and 3 orders of magnitude – Rutqvist and Stephansson, 2003). We study the extent of the EGS reservoir after the stimulation (hydrosheared zone) both in a single-phase (liquid), single-component (water) system and in a two-phase (gas, liquid), two-component (CO_2, water) system. Effects of some key parameters, such as the frictional coefficient and a permeability-enhancing factor, are studied as well.

MODEL SETUP

The coupled THM analysis was conducted using the simulator TOUGH-FLAC (Rutqvist et al., 2002; Rutqvist, 2011) based on the geothermal reservoir simulator TOUGH2 (Pruess et al., 2011), which allows the modeling of multiphase and multicomponent fluids in a porous medium, and the geomechanical code FLAC3D (Itasca, 2009), for the stress changes induced by pressure and temperature. The TOUGH-FLAC simulator has been recently applied and tested over a wide range of research fields, such as carbon sequestration (e.g., Cappa and Rutqvist, 2012; Rinaldi and Rutqvist, 2013), nuclear waste disposal (e.g., Rutqvist and Tsang, 2012, and references therein), hydrothermal systems and volcanology (Todesco et al., 2004), as well as studies related to water injection in geothermal fields (e.g., Rutqvist et al., 2013a; Vasco et al., 2013).

Following the approach of Rutqvist et al. (2013a) for modeling of the stimulation injection at the Northwest Geysers EGS Demonstration Project, we studied the stimulation at a generic EGS reservoir with low initial permeability, suitable for observing hydroshearing, such as at Newberry Volcano. Although it is beyond the aim of this paper to reproduce the data and observation recorded at the Newberry EGS Demonstration, we preferred to perform our simulation study of the hydroshearing and EGS reservoir extent starting from some reliable parameters such as those obtained from Newberry Volcano site, where data were collected for more than one year before starting the stimulation. In this study, we extended Rutqvist et al.'s (2013a) approach to calculate the actual permeability enhancement during the injection.

We considered a one-quarter symmetric model, with the injection well (corresponding to the Newberry well NWG 55-29) located in one corner (Fig. 1). The model domain is a parallelepiped of dimensions 1.5 × 1.5 × 3.5 km and consists of four layers, representing the main geological formations of the Newberry area (Sonnenthal et al., 2012). Hydrological properties are listed in Table 1.

During hydroshearing and hydrofracturing, the medium permeability changes as a result of injection-induced fluid pressure and effective stress changes, and is strongly dependent on *in situ* stress magnitude and orientation as well as fracture orientation. In this study, we consider a stress-dependent permeability (hence also an anisotropic initial permeability) with maximum permeability in the NS-direction, in order to simulate a highly fractured low permeability formation (such as the intruded John Day formation at the Newberry volcano).

The injection well was simulated as a porous medium with high vertical permeability and very high porosity). It is divided into two sections. The first section represents a cased well (high vertical permeability and very low horizontal permeability), which allow heat exchange only and prevent fluid escaping from the well to the host rock. The second section represents an open well completion (very high vertical permeability and same horizontal permeability as the host rock) that allows the injection of cold water into the highly fractured low permeability formation (between 2000 m and 3000 m depth).

Initial temperature and pressure distribution were extracted from former analyses of the pre-stimulation steady-state conditions at Newberry Volcano (Sonnenthal et al., 2012). The temperature follows a high gradient of about 100 ˚C/km, with a maximum temperature of about 360˚C at the bottom of the domain. The pressure is slightly lower than hydrostatic, with a linear gradient of about 8.3 MPa/km. Constant pressure was set at the top and bottom boundaries, whereas side boundaries were assumed to be closed to fluid flow. No-flow side boundaries are needed to simulate only a quarter of a symmetric domain.

Mechanical properties follow the results of Li et al. (2012). We chose to simulate a model with homogeneous mechanical properties and use a Young's modulus of E = 15 GPa and Poisson's ratio ν = 0.3. Homogeneous mechanical properties should be adequate in this case, since we simulate a short-term stimulation (slightly less than two months) that should affect only the injection zone (EGS reservoir). Indeed mechanical properties (such as shear and bulk modulus, and friction angle) may depend on medium heterogeneities, and then affect the stress and deformation distribution at macro scale. However, we are already accounting for an anisotropic permeability field, which affect the pore pressure distribution, and then the stress evolution as well. Random heterogeneities in mechanical properties may be present in a real field, but only at microscopic scale (i.e. too small to be analyzed in this study).

Initial geomechanical conditions follow those used by Cladouhos et al. (2011) for the pre-stimulation analysis performed with the AltaStim simulator. We considered a vertical stress gradient of 24.1 MPa/km (σ_V, maximum principal stress in *z*-direction). The intermediate principal stress is oriented in the NS-direction (*y*-axis, σ_H) with a gradient of 23.5 MPa/km. Finally, the minimum principal stress is oriented in the EW-direction with a gradient of 14.9 MPa/km (σ_h, *x*-axis). Thermal effects on stress were taken into account as well, choosing a coefficient of linear thermal expansion $\alpha_t = 10^{-5}$ °C^{-1}.

Permeability changes

Laboratory tests have shown how the state of stress may affect the hydraulic properties in samples (e.g. Liu et al., 2004). Specifically, the medium permeability is related to the fracture mechanical aperture *b* and to the effective stress normal to the fracture σ_n according to the following exponential function (Liu et al., 2004):

$$b = b_r + b_{max} \exp(\alpha \sigma_n) (1)$$

where b_r is the initial mechanical aperture, b_{max} is the mechanical aperture corresponding to zero normal stress, α is a parameter related to the curvature of the fitting function. The mechanical aperture change can also be simply related to the initial state of stress (Rutqvist et al., 2008):

$$b = b_i + b_{max} \left(\exp(\alpha \sigma_n) - \exp(\alpha \sigma_{¿}) \right) (2)$$

, and σ_{ni} is the initial stress normal to the fractures. In our formulation, compressive stresses are considered negative.

Generally most of the EGS sites feature a fracture system striking a certain direction. The Newberry Volcano, for example, features a NS-striking fracture system. Such a direction would be the *y*-axis in our formulation, and by assuming an initial anisotropic permeability field in a porous medium (higher permeability on *y*-axis), we can simulate the effects of the fracture network. The permeability would change mostly in the fracture direction (i.e. *y*-axis) and changes will be negligible in the other directions. We can calculate the changes in permeability along the *y*-direction (κ_y) as a function of the normal stress (σ_x) using the cubic law of parallel-plate flow (Witherspoon at al., 1980):

$$\kappa_y = f\frac{b_y^3}{12} \quad (3)$$

where κ_y is the permeability in the fracture direction (*y*-axis in our case) and *f* is the fracture spacing. b_y is the fracture aperture from Eq. 1 or 2, and it is a function of the stress normal to the fracture (σ_x).

Using the approach described by Eqs. 1-3 would require a high number of unknown parameters that need to be calibrated (b_r or b_i, b_{max}, *f*, and □). However, we can reduce the number of parameters by following an approach for scaling the fracture properties with the initial permeability (Liu et al., 2004). Following Eq. 3, we can relate the ratio between initial, unstressed permeability and the final permeability to the ratio between the aperture at initial state and aperture at final stage:

$$\frac{\kappa_y}{\kappa_{yi}} = \left(\frac{b_y}{b_{yi}}\right)^3 \quad (4)$$

then using a dimensionless parameter $R_b = b_r / b_{max}$, and combining Eq. 4 with Eq. 1, we can write for permeability changes (Liu et al., 2004):

$$\frac{\kappa_y}{\kappa_{yi}} = \left[\frac{R_b + \exp(\alpha \sigma_x)}{R_b + \exp(\alpha \sigma_{xi})} \right] \quad (5)$$

where the stress aperture function is related to the dimensionless parameter $R_b = b_r / b_{max}$. Assuming the fractures to be identical, R_b will be a constant through the model domain. Using R_b, the permeability change factor is independent of initial permeability. We implemented Eq. 5 into TOUGH-FLAC and calibrate our model for two parameters only (R_b and α) using data recorded during an injection test (see following section).

The variation of stress is not the only process that may affect the permeability. Most of the changes will occur after shear reactivation, which is the main mechanism for creating permanent permeability enhancement within the EGS reservoir. However, while stress-induced permeability changes occur everywhere in the domain along the direction of fractures subjected to aperture changes, the shear-induced permeability changes only occur in the portion of the domain subjected to shear reactivation. In this work we assumed that the permeability would change by a fixed factor if a gridblock were subjected to shear reactivation:

$$\kappa_i = K_{HS} \cdot \kappa_i^{bHS} \quad (6)$$

for the *i*-direction. K_{HS} is a constant value (set to 500 for the base case analyses, i.e., between 2 and 3 orders of magnitude), and the index *bHS* refers to the permeability before the hydroshearing. Reactivation may occur with random orientation if a threshold pressure is reached, then we cannot attribute the changes in a single direction, but we assume the permeability changes isotropically if shear reactivation occur.

In case of multi-stage shearing, the permeability changes accordingly, i.e. the permeability $\square^{bHS}$ represents the one before the actual shear stage.

A similar approach was also recently used by Kelkar et al. (2012) during the study of shear stimulation at Desert Peak Geothermal Field (Nevada), though limiting the permeability change to a factor of 15 upon shear failure.

Alternative approaches for modeling hydroshear may involve discrete fracture network models or combinations of fracture network and continuum models. For example when using the distinct element codes 3DEC or UDEC in which each fracture is explicitly represented, the permeability changes in individual rock fractures may be calculated as a result of aperture changes due to shear induced dilation based on some constitutive law for single fractures (e.g Min et al. 2004). Other examples involve discrete fracture network models originally developed for groundwater flow and transport extended through a simplified geomechanics approach in which shear failure on each fracture is evaluated in an assumed and constant and homogenous external stress field (e.g. Willis-Richards 1996; Bruel, 2007). In such an approach, the fracture responses upon shear failure may be calculated based on a local elastic solution for an assumed circular shaped fracture of certain radius. For example, based on the radius of the fracture and shear modulus of the surrounding rocks, the shear stress drop and maximum shear displacement and associated fracture dilation and permeability change can be calculated. Such an approach has the potential of handling a large number of fractures explicitly, but the mechanics is simplified as described and does not consider shear induced stress changes or relaxation of the stress field in stimulated areas. A combination approach may involve considering a back-ground fracture network used for calculating equivalent continuum properties that for a very fine continuum mesh can be used to represent fractures explicitly by changing properties of elements that are intersected by individual fractures surfaces (Tezuka et al., 2005; Rutqvist et al., 2013b). The approach for permeability change adopted in this study can be considered a rational approach applied to a continuum model. However, regardless of the model adopted it usually involves some level of calibration against field data as will be discussed in the next section.

Model calibration

Model calibration is necessary for understanding whether the system is correctly responding to the injection of fluids and whether boundary and initial conditions are properly set.

Pore compressibility (c_p) and thermal conductivity (□) within the injection well were calibrated to match field data. Moreover, a calibration is needed to assign appropriate values to the parameters □ and R_b for the stress-dependent permeability function (Eq. 5).

The calibration was made simulating a low-pressure injection test, and comparing the resulting pressure and temperature profiles along the well with data collected at the NWG 55-29 well during a field injection test (September-October 2010).

According to Davatzes and Hickman (2011) the injection test was performed in two steps. During the first period, lasting three days, the injection rate was 0.6 L/s (10 gpm) with an injection temperature of 10˚C and a well-head pressure of about 5 MPa (750 psi). This period was then followed by two weeks of shut-in, before restarting the injection for nine days at a rate of 1.4 L/s (22 gpm), with an injection temperature of 10˚C and a wellhead pressure of about 8 MPa (1153 psi).

Here we performed a simulation with the same, transient injection and we reproduced the same observed profiles along the well for pressure and temperature after 3 days at 10 gpm (Fig. 2a and b for pressure and temperature, respectively) and after 9 days at 22 gpm (Fig. 2c and d, for pressure and temperature, respectively), considering the permeability changes that may arise with the evolving effective stresses. Parameters for permeability changes were set constant during the two stages as $R_b = 0.2$ and = 0.13 MPa^{-1} after calibration (see Eq. 5). The calibration for R_b and is not unique, but the used of the two parameters only reduce the degree of freedom of the system.

The pore compressibility and thermal conductivity were calibrated as well, and the values allowing a good match between simulated and measured profiles are listed in Table 1. As stated by Davatzes and Hickman (2011), after nine days of 22 gpm injection the well-head pressure was lowered to allow the well to be logged; hence, the pressure field data in Figure 2d needs to be recalibrated to match a wellhead pressure of 8 MPa (1153 psi) during the majority of the inject-to-cool operation.

STIMULATION AND HYDROSHEARING MODELING

The stimulation of an EGS reservoir requires that an elevated amount of water be injected into the system. For example, at the Basel geothermal system (Switzerland) more than 11500 m^3 of water were injected in about 5 days (about 30 L/s average flow rate) before peaking at a well-head pressure of almost 30 MPa and inducing a $M_L = 3.4$ event (Bachmann et al., 2011). In contrast, at the Northwest Geysers EGS Demonstration at The Geysers Geothermal Field (California), flow rates reached more than 50 L/s, but bottom-hole pressures were relatively low (typically less than 8 MPa), resulting in a large number of small-magnitude seismic events and a maximum magnitude event of 2.87 (Garcia et al., 2012; Vasco et al., 2013; Rutqvist et al. 2013a). Flow rates during the stimulation at the Newberry EGS Demonstration ranged from about 5 L/s up to 20 L/s, with a well-head pressure that peaked at about 16 MPa (Fig. 3, Petty et al., 2013). The stimulation was conducted in three different stages, and thermally degradable zonal isolation materials (TZIM) were injected between each stage to partially seal stimulated permeable fractures and activate stimulation in a new zone. The use of chemical diverters (TZIM) helped to stimulate multiple zones in the well bore, resulting then in a more injection or flow capacity (last ten days in Fig. 3). Detailed description of the three stages performed during the stimulation can be found in Petty et al. (2013).

Here we are interested in the effects of the stimulation on hydroshearing and how far EGS reservoirs can extend under different system conditions. In most of the EGS applications, operators try to maintain a fixed injection rate, monitoring the injection pressure as outcome. However, we preferred to keep the pressure constant rather the injection rate, since the pressure is the main variable for reactivation. There was no fundamental reason, and it was done for better understanding of the process of hydroshearing, which is mainly based on pressure rather than on the flow rate. The stimulation injection is simulated by fixing the pressure at the top of the well, following the average values recorded at the Newberry Volcano EGS Demonstration. Again, it is not our goal to reproduce the observed injectivity and flow rates in detail, but it is essential to keep our model as close as possible to a real case, in order to achieve reasonable simulation results (Fig. 3).

We simulated the injection in two stages. The first stage lasted for about 28 days with a fixed well-head pressure of 7.8 MPa. This is followed by a 10 day shut-in period, before the injection restarts for the second stage with 3 days at 7 MPa and 10 days at 14 MPa (Fig. 3, green line). Note that we did not consider the effect of diverters (TZIM), which means that an increase in pressure results in an increase in flow rate, whereas, as observed at Newberry, the diverters sealed the permeable zones, permitting an higher well-head pressure without a substantial increase in flow rate prior to the start of subsequent stimulation steps.

The increase in pressure is necessary to allow the system to reduce the shear strength of fractures to less than the shear stress across the fracture, and enable the hydroshearing of fractures with a wider variety of fracture orientations to occur (Cladouhos et al, 2011). Rather than keeping a fixed, high value for the well-head pressure, we preferred to study a case of transient evolution, in which the injection starts at a relatively low pressure (7 MPa, first stage) and then is doubled after a shut-in (no-injection) period (14 MPa, second stage). The values we chose are within the range needed for hydroshearing, but never exceeded the minimum principal stress, so that only shear failure can occur, rather than tensile failure or fracturing.

To estimate the extent of the EGS reservoir, we looked at the zone where the system is subjected to hydroshearing. This can be done with a Mohr-Coulomb model: considering a cohesionless solid, shear reactivation will occur when the following criterion is satisfied:

$$\sigma'_{1c} = N_\phi \sigma'_3, N_\phi = \frac{1+\sin\phi}{1-\sin\phi} \quad (7)$$

where σ'_{1c} is the critical maximum principal effective stress (σ'_V or σ'_{zz} in our case), and σ'_3 is the minimum principal effective stress (σ'_h or σ'_{xx}). ϕ is the frictional angle (frictional coefficient $\mu=\tan\phi$), which is set to 30° for the base-case simulation. In our model we considered as Mohr-Coulomb solid the Intruded John Day formation only, and the upper John Day formation, which is not a highly fractured formation, acts as a barrier for fracture propagation (Fig. 1). This may not be true in the field, and the fractures may propagate to shallow depth.

Equation 7 corresponds to the case in which the media contains fractures with a uniform distribution of orientations and equally spaced throughout the reservoir. Using this approach, shear reactivation would be induced whenever the maximum principal stress is N_ϕ times higher than the minimum principal stress.

Stimulation of a single phase, single component system

The first model we analyze does not take into account the presence of gas within the system. Basically, we simulated the stimulation of a geothermal system injecting water into a fully water-saturated system. We are fully aware that this is a limiting case in this high temperature environment, but would certainly be applicable in lower temperature systems. For this base case the friction angle ϕ was set to 30˚, i.e., a standard value corresponding to a frictional coefficient of about 0.6. The constant K_{HS} for shear-enhanced permeability changes was set to 500, i.e. corresponding to a 2.7-order magnitude change in permeability to all directions when a shear reactivation occurs. This constant was set to a sensible value (Rutqvist and Stephansson, 2003). For example, Lee and Cho (2002) have shown after laboratory tests that two orders magnitude increase in fracture permeability may arise upon shear displacement.

Figure 4a shows the pressure transient evolution applied at the top of the injection well (red line) and the resulting flow rate associated with the water-saturated system (blue line). Results show a first period during which the flow rate increases up to about 30 kg/s, then hydroshearing begins occurring and the flow rate stabilizes to a constant value of about 20 kg/s (or L/s) for the rest of the first stage (0 – 28 days with well-head pressure at 7.8 MPa). During the 10 day shut-in period, the flow rate is almost nil. Then, during the second stage of stimulation, the well-head pressure reaches 14 MPa, and the flow rate peaks at more than 60 kg/s, only to decrease to 40 kg/s at the end of the stimulation. The simulated flow rates are similar to values observed at EGS demonstration sites such as The Geysers (Rutqvist et al., 2013a; Vasco et al., 2013) and Newberry Volcano (Petty et al., 2013). Again, note that we are not simulating any injection of diverters, and then, during our second stage of the stimulation for a higher well-head pressure, we achieve a higher flow rate. The use of diverters proved to be effective at Newberry, where the sealing properties of the injected isolating materials sealed the existing permeable fracture network, thus resulting in higher pressures but with the same flow rate (Petty et al., 2013).

Results for pressure changes within the system, and the resulting zone affected by shear reactivation after 28 days of stimulation, are shown in Figure 4b and c, respectively. Pressure changes and the hydrosheared zone both extend up to about 400 m from the injection well in the NS direction (*y*-axis), i.e., along the direction we set as the primary fracture strike, which has higher permeability (Table 1). Growth of the hydrosheared zone is much smaller in the EW direction (*x*-axis), since both the initial permeability and the stress-induced permeability changes are smaller in the EW direction, which means that pressure changes do not propagate much in that direction. Although the pressurization within the well reaches about 8 MPa (same as the wellhead pressure during this first stage), within the system the pressure changes are a few MPa smaller, reaching a maximum of 6 MPa at the bottom of the well (Fig. 4b). However, these few MPa changes are enough to satisfy the failure criterion and activate the shearing process (Fig. 4c).

After the second stage, the increased well-head pressure results in higher-pressure changes within the system. In fact, Figure 4d shows the changes to be around 6 MPa, with maximum value of 8 MPa in the region close to the bottom of the well, although these values are still a little smaller than the pressure change within the well (about 12 MPa). The resulting hydrosheared region expands somewhat during the second stage, reaching a maximum value of about 500 m along the NS-direction (Fig. 4e). We can estimate the extent of the EGS reservoir and calculate the volume of the region affected by pressure change and where reactivation occurred: such a stimulated volume corresponds to about $9 \cdot 10^7$ m^3, i.e., about 0.1 km^3.

Stimulation of a two phase, two component system

In this section, we consider a system that before the stimulation is completely dry, saturated with gaseous CO_2, subjected to cold-water injection. Hydrological and mechanical properties were kept the same as the fully water-saturated case. We used an equation of state for a two-components system (CO_2 and water – EOS2). Carbon dioxide can dissolve in water according to the Henry’s law and the equation of state is applicable up to the water critical temperature (350

°C), although it does not account for chemical reaction. More details can be found elsewhere (Pruess et al., 2011).

This conceptual model may be somewhat unrealistic, but it represents a good case study as compared to the previous water-saturated system. Moreover, CO_2 is a good approximation for a volcanic gas: there are a few examples in literature of CO_2 degassing in volcanic regions, such as Campi Flegrei caldera (Italy) (e.g. Todesco et al., 2004) or Furnas (Azores) (e.g. Rinaldi et al., 2012). As previously implemented, we set the friction angle to 30° and the shear-enhanced permeability-changes factor to 500.

Results of the stimulation for this system involving two fluid phases and two fluid components are shown in Figure 5. The pressure transient evolution imposed at the well is the same as previously (red line, Fig. 5a), and only a few changes are evident in the resulting flow rate compared to the case of a water-saturated system (blue line, Fig. 4a and 5a). The small variations are at the beginning of the simulation, during which a system with gas requires a higher flow rate to displace the gas from the region close to the injection well.

The resulting pressure increase after the first stage (28 days) is still close to the injection well, with an average value of about 5 MPa (Fig. 5c). Although the pressure changes do not propagate far from the injection well, the average variation is still similar to the previous water-saturated case (Fig. 4b). As a consequence of the poorly distributed pressure changes, at this stage the region affected by hydroshearing is limited to a small region around the injection well and extends only for about 60 m along NS direction and 13 m along EW direction (Fig. 5d).

After the second stage (51 days), the pressure changes are still averaging around 5 MPa, although within the well the pressure is 14 MPa (Fig. 5d). In any case, at this stage the pressure perturbation propagated more, resulting in a larger region where the shear reactivation occurred.

The hydrosheared region extends about 100 m along the NS direction and about 25.5 m along the EW direction (i.e., almost twice that after the first stage, Fig. 5e).

The results suggest that fractures will propagate much less in a medium initially saturated with a compressible gas. In fact, the stimulated volume resulting for an unsaturated medium is about 10^7 m^3, i.e., about 1 order magnitude smaller than the volume that can be stimulated in a medium fully saturated with water. This effect can be explained because of the compressibility of the gas phase. In a saturated medium, the water within the system is pushed away from the volume that is injected, allowing for the pressure perturbation to move faster, thus reactivating a larger region. In an unsaturated medium, the gas phase will be compressed by the injected water. The injected water will propagate only to a region close to the injection well, with the pressure perturbation following the water front, resulting in the stimulation of a much smaller region.

Thermal effects on hydroshearing

The injection of cold water produces changes in temperature distribution. The changes are mostly confined around the injection well, and extend only a few tens of meters, with changes up to more than 30 ˚C. Resulting temperature distribution for both the water-saturated and unsaturated cases are shown in Figure 6a and c, respectively. Although we have seen how the hydrosheared zone can differ between a water-saturated and an unsaturated system, changes in temperature are very similar, as already showed for the resulting flow rates (Fig. 4a and Fig. 5a). However, these small and confined changes in temperature may have an effect on the resulting stress. In essence, the cooling caused by the injection along the permeable (stimulated) zone causes cooling shrinkage that in turn tends to cause an additional reduction in effective stress and shear strength. Such shear strength reduction will tend to promote shear failure and propagation of the stimulation zone. In fact, if we compared a case that considered a hydro-mechanical (HM, i.e. considering $\square_t = 0$) coupling only with a full THM modeling, we found that the temperature changes may help the EGS reservoir growth. In fact, the when conspiring thermal effects, EGS reservoir grow about 100 m farther along the NS direction for the case of water-saturated system (Fig6b, THM brown, HM yellow). Some small differences are observed for the case of gas-saturated system, with about 20 m difference between THM and HM modeling, with a slightly larger reservoir when thermal effects are taken into account (Fig6d).

Sensitivity analysis

We have seen how two systems can respond differently to stimulation if we account for the presence of gas. However, the presence of gas within a system is only one of the parameters that should be taken into account when simulating a complex system such as a geothermal reservoir. Some of the parameters can be taken from field studies: for example, the stress field, which plays a huge role in shear reactivation, can be evaluated by *in situ* tests, and by looking at local seismicity. The same can be done for the permeability, although most of the parameters studied in the laboratory analysis can produce results quite different from those observed in the field. Here, we aim to focus only on two main parameters that affect the resulting stimulated volume: (1) the constant K_{HS} for the shear-enhanced permeability (Eq. 6) and (2) the frictional angle ϕ for the Mohr-Coulomb criterion (Eq. 7). All the analyses presented in this section were done at the end of the second stage, i.e., after 51 days of simulation.

In the base-case simulations we set a shear-enhanced permeability change factor to achieve between a 2 and 3 orders magnitude change (K_{HS} = 500). However, in the field this factor may be greater (or smaller), leading to a different system response. Figure 7a shows how the EGS reservoir extent varies along the NS direction as a function of this constant for both an unsaturated (red line) and saturated system (blue line). Figure 7b shows the stimulated volume as a function of the shear-enhanced permeability factor. The extent of the region subject to hydroshearing may reach up to 800 m in a water-saturated system, when we consider a factor 10^4

of permeability changes, or may extend for few tens of meters when we do not consider changes in permeability due to hydroshearing (K_{HS} = 0). These variations are much smaller for an unsaturated system. Even if we use a factor 10^4, in a system that is initially gas-dominated, the reservoir may extend up to about 200 m only. From both Figures 7a and b, we found that the hydrosheared region (extent or volume) varies as a logarithmic function of the shear-enhanced permeability factor greater than 10 (i.e. $\log_{10}(K_{HS})$ greater than one):

$$V_{HS}(L_{EGS})\ \ \log_{10}(K_{HS})(K_{HS})(5)$$

where V_{HS} represents the volume subjected to hydroshearing, which is proportional to the EGS reservoir length (L_{EGS}). Note the logarithmic scale that Figure 7b.

The second parameter for which we perform a sensitivity analysis is the friction angle. For the base-case simulations, we used an angle of 30°, which means a friction coefficient of about 0.6. This factor can play a big role, depending upon the initial stress condition. Considering a fixed, linear stress distribution, with no heterogeneities and variation in depth, the friction angle simply regulates how much overpressure is needed to satisfy the failure criterion (Eq. 7). Results of the sensitivity analysis for this parameter are shown in Figures 6c and d, for the EGS extent along the NS direction and for the stimulated volume, respectively. Both these variables seem to change linearly with the friction angle, with values ranging between 600 m (volume $2 \cdot 10^8$ m^3) and 250 m (volume $5 \cdot 10^7$ m^3) for a water-saturated medium with an increase in the friction angle resulting in a smaller stimulated volume and linear extent, and hydrosheared region is almost costant for an unsaturated medium: only a 40 m variation in EGS extent over the considered range of values.

CONCLUSIONS

During stimulation of an Enhanced Geothermal System (EGS) it is always difficult to predict how far the reservoir and fracture network can grow. Moreover, creating a new fracture network requires elevated pumping pressure and flow rates in order to fracture the rock. One mechanism that has been proposed to reduce the cost is so-called *hydroshearing*, which involves reactivating an existing fracture network by a shear process, taking advantage of the fracture surface roughness, which should naturally maintain the enhanced permeability. The pressure needed for hydroshearing has to be below the minimum principal stress, but without exceeding it, thus avoiding then the creation of new tensile fractures. Once the fractures are reactivated, some isolating, thermally degrading material may be injected to plug the fracture network, and this will permit stimulating multiple fracture zone without drill rig or setting multiple packers. Moreover, the injection of chemical diverters will permit injecting at a higher pressure (hence reactivating some other, deeper zones) without changing the flow rate.

However, some questions need to be answered: will the presence of gas within the system help or reduce the hydroshearing reactivation? How much can the permeability change after reactivation, and how is that change related to the extent of the EGS reservoir and to the stimulated volume? The aim of this paper was to answer to these questions. Through the use of the TOUGH-FLAC simulator, we carried out a coupled thermo-hydro-mechanical modeling of EGS stimulations. We accounted for a Mohr-Coulomb solid that can fail when a criterion is satisfied. Upon fracture reactivation, we assumed a change in medium permeability, which allows for a better propagation of the pressure perturbation. Taking into account previous simulations performed for

The Geysers Geothermal Field and starting with data collected at the Newberry Volcano EGS Demonstration site, we simulated the stimulation by fixing the overpressure at the top of an injection well. Pressure transient evolution was taken as the average of field values measured at Newberry Volcano during stimulation. Although our aim was not to reproduce any observed variations, we used field data to keep our model as realistic as possible.

We first presented the results for two limiting cases: (1) a water-saturated medium and (2) a medium initially saturated with CO_2 in the gas phase. Results suggest that an EGS reservoir will extend much further in a medium initially fully saturated with water than in a gas-phase dominated system. We explained this effect as owing to the compressibility of the gas phase. In a water-saturated medium, the native water within the system is pressurized by the water injected into the well, allowing the pressure perturbation to propagate faster and reactivating fractures over a larger region. In an unsaturated medium, the much more compressible gas phase will be compressed by the injected water, which will propagate only to a region close to the injection well, following the water front, finally stimulating a much smaller region. Thermal effects on stress may help to reach shear failure. Although temperature changes are small and confined within tens of meter from the injection well, thermal effects on stress are evident at earlier time and helped the EGS reservoir to grow. A hydro-mechanical modeling resulted in smaller hydrosheared region after the stimulation.

The presence of gas is not the only parameter affecting the growth of an EGS reservoir. Many parameters are involved that may play a significant role, such as the medium initial permeability, the natural fracture-network orientation, and the stress distribution. We performed a sensitivity analysis on two key parameters that are generally hard to measure in the field: (1) the factor for the shear-enhanced permeability changes and (2) the friction angle for the failure criterion. Results showed that the extent of the EGS reservoir and the volume subjected to shear reactivation strongly depend upon these two parameters. We found that in our system, the EGS extent (or reactivated region volume) will depend logarithmically upon the constant used to relate permeability change associated with hydroshearing, and linearly upon the frictional angle. These variations are more accentuated in a water-saturated system.

The volume subjected to hydroshearing (stimulated volume) ideally should also represent the region where the microseismicity cloud should be. However, natural-system heterogeneities in the stress field and permeability may play a significant role, and the seismicity cloud may not exclusively represent only the region that has been stimulated. For example, a brittle material at shallow depth may be affected by deformation and stress transfer coming from a deeper overpressure, and seismicity may then be induced at a shallower depth than we would expect. Technical issues may be involved as well: for example, a leakage from the cased well may allow the water to move at shallow depths, where it is much easier to cause hydroshearing, or hydrofracturing, since the *in situ* would be stress smaller, generally depending on the depth.

ACKNOWLEDGMENTS

This work was supported by the Department of Energy under Award Number DE-EE0002777 and by the American Recovery and Reinvestment Act (ARRA), through the Assistant Secretary for Energy Efficiency and Renewable Energy (EERE), Office of Technology Development, Geothermal Technologies Program, of the U.S. Department of Energy under contract no. DE-AC02-05CH11231. Technical review comments by Matt Uddenberg of the AltaRock company, and Patrick F. Dobson and Pierre Jeanne at the Berkeley Lab, as well as editorial review by Dan Hawkes at the Berkeley Lab are all greatly appreciated.

REFERENCES

Bachmann, C. E., S. Wiemer, J. Woessner, S. Hainzl, Statistical analysis of the induced Basel 2006 earthquake sequence: Introducing a probability-based monitoring approach for Enhanced Geothermal System, *Geophys. J. Int.*, 186(2) (2011). doi:10.1111/j.1365-246X.2011.05068.x.

Baria R, Baumgärtner J, Rummel F, Pine RJ, Sato Y (1999a) HDR/HWR reservoirs: concepts, understanding and creation. Geothermics 28:533–552.

Bruel, D., 2007, Using the migration of the induced seismicity as a constraint for fractured hot dry rock reservoir modeling: International Journal of Rock Mechanics and Mining Sciences & Geomechanics Abstracts, 44, 1106–1117.

Cappa, F., J. Rutqvist, Seismic rupture and ground accelerations induced by CO_2 injection in the shallow crust, *Geophys. J. Int.*, 190, 1784-1789 (2012).

Cladouhos, T. T., M. Clyne, M. Nichols, S. Petty, W. L. Osborn, L. Nofziger, Newberry Volcano EGS Demonstration Stimulation Modeling, *GRC Transactions*, 35 (2011).

Cladouhos, T. T., W. L. Osborn, S. Petty, D. Bour, J. Iovenitti, O. Callahan, Y. Nordin, D. Perry, P. L. Stern, Newberry Volcano EGS Demonstration – Phase I results, *Proceedings of 37th Workshop on Geothermal Reservoir Engineering*, Stanford, California, January 30 – February 1, 2012.

Cladouhos, T. T., S. Petty, B. Larson, J. Iovenitti, B. Livesay, R. Baria, Toward More Efficient Heat Mining: A Planned Enhanced Geothermal System Demonstration Project, *GRC Transactions*, 33, 165-170 (2009).

Cladouhos, T. T., S., Petty, Y. Nordin, M. Moore, K. Grasso, M. Uddenberg, M. Swyer, B. Julian, G. Foulger, Microseismic Monitoring of Newberry Volcano EGS Demonstration, *Proceedings of the 38th Workshop on Geothermal Reservoir Engineering*, Stanford, California, February 11 - 13, 2013.

Davatzes N. C. and S. H. Hickman, Preliminary Analysis of Stress in the Newberry EGS Well NWG 55-29, *GRG Transactions*, 35, 323-332 (2011).

Evans KF, Cornet FH, Hashida T, Hayashi K, Ito T, Matsuki K, Wallroth T (1999) Stress and rock mechanics issues of relevance to HDR/WDR engineered geothermal systems: review of developments during the past 15 years. Geothermics 28:455–474

Garcia, J., Walters, M., Beall, J., Hartline, C., Pingol, A., Pistone, S., and Wright, M., Overview of the Northwest Geysers EGS demonstration project, *Proceedings of the 37th Workshop on Geothermal Reservoir Engineering*, Stanford, California, January 30 – February 1, 2012

Kelkar, S., K. Lewis, S. Hickman, N. C. Davatzes, D. Moos, G. Zyvoloski, Modeling coupled thermal-hydrological-mechanical processes druing shear stimulation of an EGS well, *Proceedings of the 37th Workshop on Geothermal Reservoir Engineering*, Stanford, California, January 30 - February 1, 2012.

Lee, H. S., and T. F. Cho, Hydraulic Characteristic of Rough Fractures in Linear Flow under Nomrla and Shear Load, *Rock Mech. Rock Eng.*, 35 (4), 299-318, 2002.

Li, Y., J. Wang, W. Jung, A. Ghassemi, Mechanical Properties of Intact Rock and Fractures in Welded Tuff from Newberry Volcano, *Proceedings of 37th Workshop on Geothermal Reservoir Engineering*, Stanford, California, January 30 – February 1, 2012.

Liu, H. H., J. Rutqvist, G. Zhou, G. S. Bodvarsson, Upscaling of normal stress-permeability relationship for fracture network obeying the fractional levy motion. In: Stephansson O., Hudson J. A., Jing L., editors. *Coupled THMC processes in geo-system: fundamentals, modelling, experiments and applications*. Oxford: Elsevier; p.263-268 (2004).

Itasca, *FLAC3D, Fast Lagrangian Analysis of Continua in 3 Dimensions, Version 4.0*, Minneapolis, Minnesota, Itasca Consulting Group (2009).

Makurat A, Barton N, Rad NS (1990) Joint conductivity variation due to normal and shear deformation. In: Barton N, Stephansson O (eds) Rock joints. Balkema, Rotterdam, pp 535–540

Min KB, Rutqvist J., Tsang C.-F., and Jing L. Stress-dependent permeability of fracture rock masses: a numerical study. *Int. J. Rock Mech. & Min. Sci*, 41, 1191-1210 (2004).

Petty, S., Y. Nordin, W. Glassley, T. T. Cladouhos, M. Swyer, Improving Geothermal Project Economics with Multi-Zone Stimulation: Results from the Newberry Volcano EGS

Demonstration, *Proceedings of the 38th Workshop on Geothermal Reservoir Engineering*, Stanford, California, February 11 - 13, 2013.

Pine RJ, Batchelor AS (1984) Downward migration of shearing in jointed rock during hydraulic injections. Int J Rock Mech Mining Sci 21:249–263

Pruess, K., C. M. Oldenburg, and G. Moridis, *TOUGH2 User's Guide, Version 2.1*, Report LBNL-43134 (revised), Lawrence Berkeley National Laboratory, Berkeley, Calif. (2011).

Riahi, A., B. Damjanac, Numerical Study of Hydro-Shearing in Geothermal Reservoirs with a Pre-Existing Discrete Fracture Network, *Proceedings of the 38th Workshop on Geothermal Reservoir Engineering*, Stanford, California, February 11 - 13, 2013.

Rinaldi, A. P., J. Rutqvist, Modeling of deep fracture zone opening and transient ground surface uplift at KB-502 CO_2 injection well, In Salah, Algeria, *Int. J. Greenh. Gas Contr.*, 12, 155-167 (2013). doi:10.1016/j.ijggc.2012.10.017.

Rinaldi, A. P., J. Vandemeulebrouck, M. Todesco, F. Viveiros, Effects of atmospheric conditions on surface diffuse degassing, *J. Geophys. Res. - Solid Earth*, 117, B11201 (2012). doi:10.1029/2012JB009490.

Rutqvist, J., Status of TOUGH-FLAC simulator and recent applications related to coupled fluid flow and crustal deformations. *Comput. Geosci.*, 37, 739-750 (2011).

Rutqvist J., Dobson P.F., Garcia J., Hartline C., Jeanne P., Oldenburg C.M., Vasco D.W., Walters M. The Northwest Geysers EGS Demonstration Project, California: Pre-stimulation Modeling and Interpretation of the Stimulation. Mathematical Geosciences, In press, (2013a)

Rutqvist J., Leung C., Hoch A., Wang Y., and Wang Z. Linked multicontinuum and crack tensor approach for modeling of coupled geomechanics, fluid flow and transport in fractured rock. International Journal of Rock Mechanics and Geotechnical Engineering, 5, 18–31 (2013b)..

Rutqvist, J., B. Freifeld, K.-B. Min, D. Elsworth, Y. Tsang, Analysis of thermally induced changes in fractured rock permeability during 8 years of heating and cooling at the Yucca Mountain Drift Scale Test, *Int. J. Rock Mech. Min. Sc.*, 45, 1373-1389 (2008).

Rutqvist, J., O. Stephansson, The role of hydromechanical coupling in fractured rock engineering, *Hydrogeology Journal*, 11 (1), 7-40 (2003).

Rutqvist, J., C. F. Tsang, Multiphysics processes in partially saturated fractured rock: Experiments and models from Yucca mountain, *Rev. Geophys.*, 50(3) (2012). doi:10.1029/2012RG000391.

Rutqvist, J., Y.-S. Wu, C.-F. Tsang, G. Bodvarsson, A modeling approach for analysis of coupled multiphase fluid flow, heat transfer, and deformation in fractured porous rock, *Int. J. Rock Mech. Min. Sc.*, 39, 429-442 (2002).

Sonnenthal, E. L., N. Spycher, O. Callahan, T. Cladouhos, and S. Petty, A thermal-hydrological-chemical model for the Enhanced Geothermal System Demonstration Project at Newberry Volcano, Oregon, *Proceedings of the 37th Workshop on Geothermal Reservoir Engineering*, Stanford, California, January 30 - February 1, 2012.

Tester, J.W. et al., 2006 The future of geothermal energy. Part 1—Summary and part 2—Full report. Massachusetts Institute of Technology, Cambridge, MA.

Tezuka K., Tamagawa T., and Watanabe K. 2005. Numerical Simulation of Hydraulic Shearing in Fractured Reservoir. Proceedings World Geothermal Congress 2005. Antalya, Turkey, 24-29 April 2005

Todesco, M., J. Rutqvist, G. Chiodini, K. Pruess, C. M. Oldenburg, Modeling of recent volcanic episodes at Phlegrean Fields (Italy): geochemical variations and ground deformation, *Geothermics*, 33, 531-547 (2004).

Vasco, D. W., J. Rutqvist, A. Ferretti, A. Rucci, F. Bellotti, P. Dobson, C. M. Oldenburg, J. Garcia, M. Walters, C. Hartline, Monitoring deformation at The Geysers geothermal field, California using C-band and X-band Interferometric Synthetic Aperture Radar, *Geophys. Res. Lett.*, accepted for publication (2013). doi:10.1002/grl.50314.

Willis-Richards, J., K.Watanabe, and H. Takahashi, 1996, Progress toward a stochastic rock mechanics model of engineered geothermal systems: Journal of Geophysical Research, 101, 17, 481–17, 496.

Witherspoon, P. A., J. S. Y. Wang, K. Iwai, J. E. Gale, Validity of cubic law for fluid flow in a deformable rock fracture, *Water Resour. Res.*, 16, 1016-1024 (1980).

Ziagos J., Phillips B.R., Boyd L., Jelacic A., Stillman G. and Eric Hass E. A technology roadmap for strategic development of enhanced geothermal systems. Proceedings of the 38^{th} Workshop on Geothermal Reservoir Engineering , Stanford, California, February 11 - 13, 2013.

Tables

Table 1. Hydrological properties. □$_i$ initial (stress-free) permeability along *i*-direction. □ porosity. □$_{rock}$ rock density. *D* rock grain specific heat. □ thermal conductivity. c_p pore compressibility

	Newberry-Deschutes	John Day	Intruded John Day	Cased well	Open well
□$_x$ (m^2)	10^{-17}	$2.6 \cdot 10^{-16}$	$5 \cdot 10^{-18}$	10^{-20}	10^{-16}
□$_y$ (m^2)	10^{-17}	$2.6 \cdot 10^{-16}$	10^{-17}	10^{-20}	10^{-16}
□$_z$ (m^2)	10^{-17}	$2.6 \cdot 10^{-16}$	$5 \cdot 10^{-18}$	10^{-8}	10^{-8}
□□□□□	10	5	3	95	100
□$_{rock}$ (kg/m^3)	2400	2400	2400	-	-
D (J/kg ˚C)	1000	1000	1000	800	800
□□(W/m ˚C)	1.80	2.15	2.20	2.20	1.80
c_p (Pa^{-1})	$3.2 \cdot 10^{-9}$	$3.2 \cdot 10^{-9}$	$3.2 \cdot 10^{-9}$	-	-

Figure captions

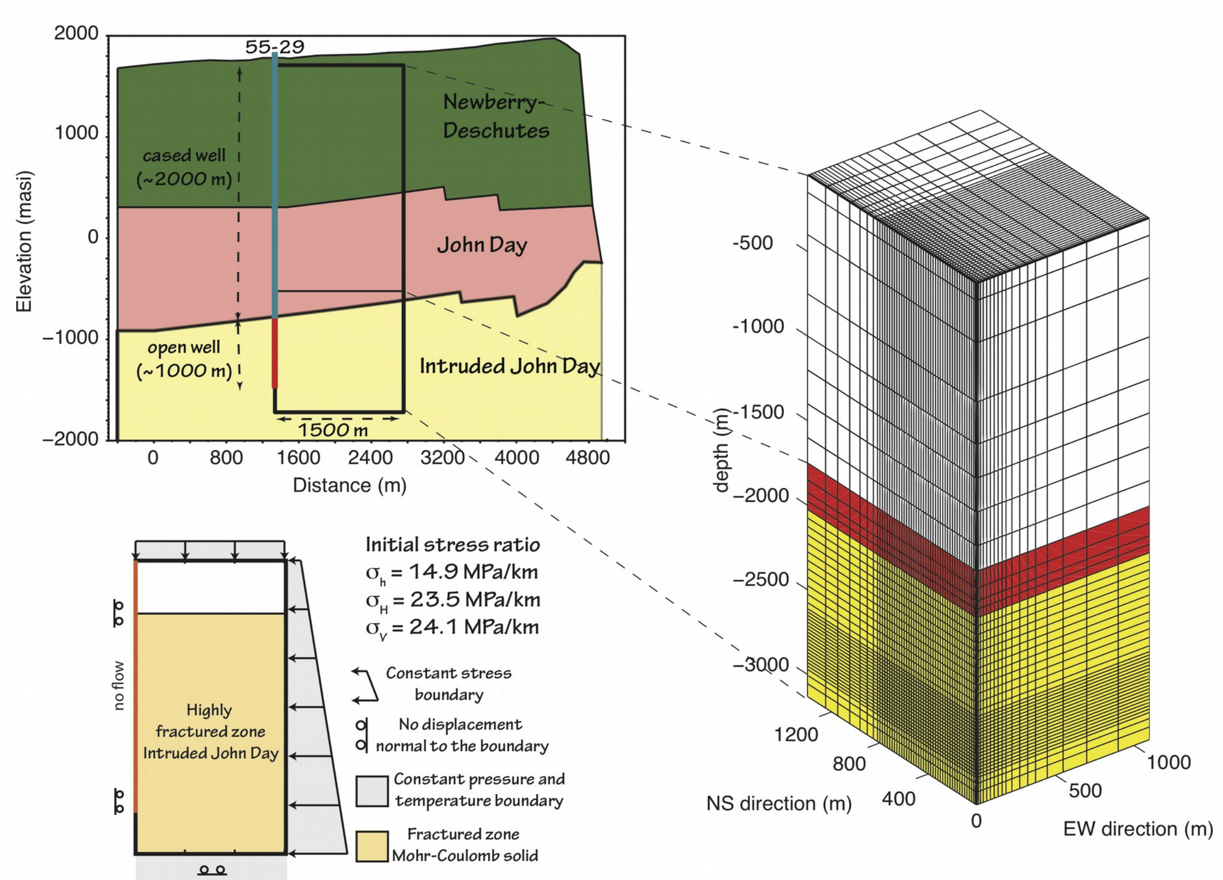

Figure 1. Mesh and boundary conditions for modeling the stimulation of an EGS reservoir. Initial pressure, temperature and stress condition follows pre-stimulation analysis at the Newberry Volcano EGS Demonstration, as well as rock properties and distribution.

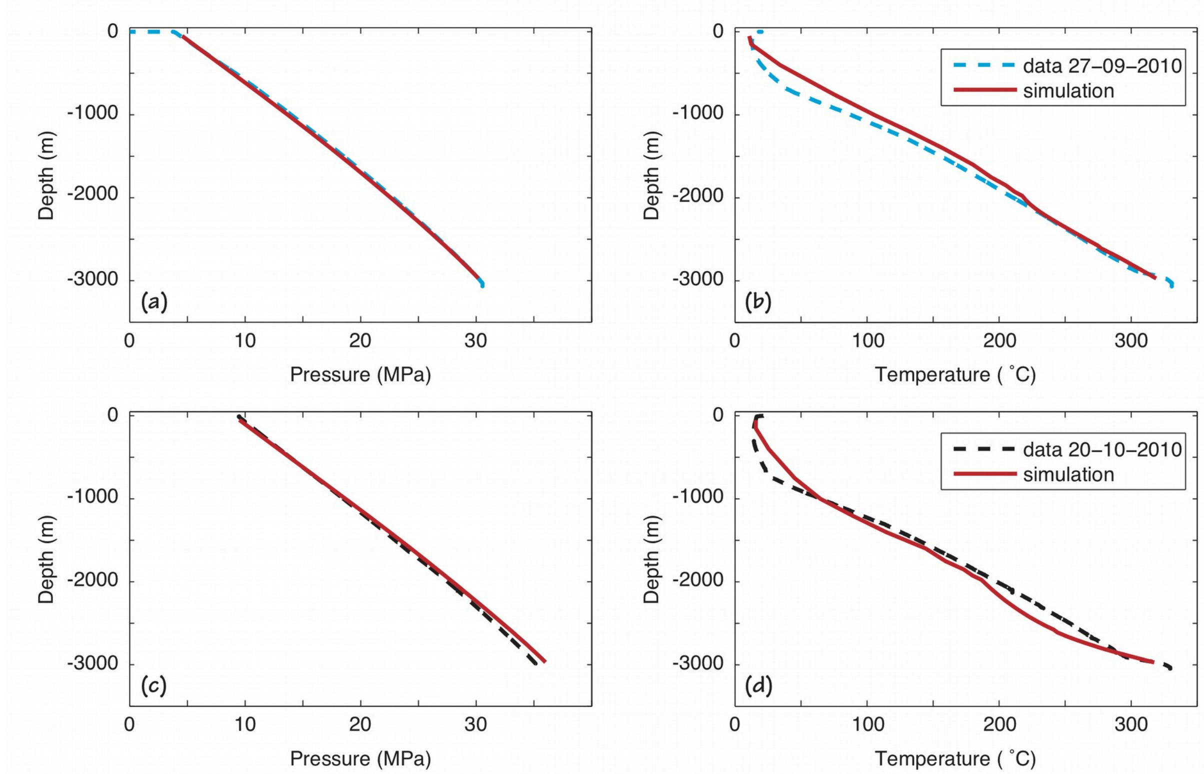

Figure 2. Model calibration. (a) Pressure well log (blue, dashed line) and simulated pressure (red line) after 3 days (09/27/2010) of 0.6 kg/s (10 gpm) injection rate. (b) Temperature well log (blue, dashed line) and simulated temperature (red line) after 3 days (09/27/2010) of 0.6 kg/s (10 gpm) injection rate. (c) Pressure well log (black, dashed line) and simulated pressure (red line) after 9 days (10/20/2010) of 1.4 kg/s (22 gpm) injection rate. (d) Temperature well log (blue, dashed line) and simulated temperature (red line) after 9 days (10/22/2010) of 1.4 kg/s (22 gpm) injection rate.

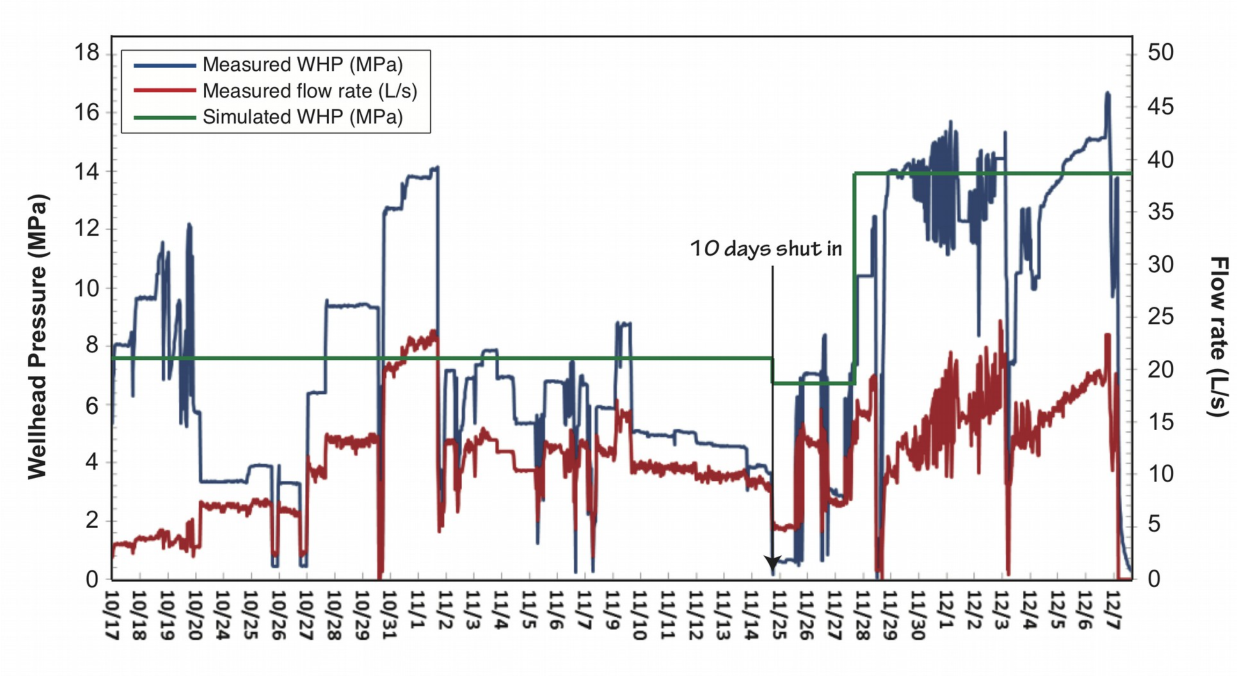

Figure 3. Example of stimulation. Wellhead pressure (blue) and injection rate (red) observed at Newberry Volcano EGS Demonstration. Gap in timeline is when stimulation pumps were offline. The green line represents an average of the wellhead pressure, which is used as input for our modeling of an EGS system to study the hydroshearing. The shut in period between our first and second stage is indicated in figure. Note that at Newberry during that period the injection continued at a very low rate.

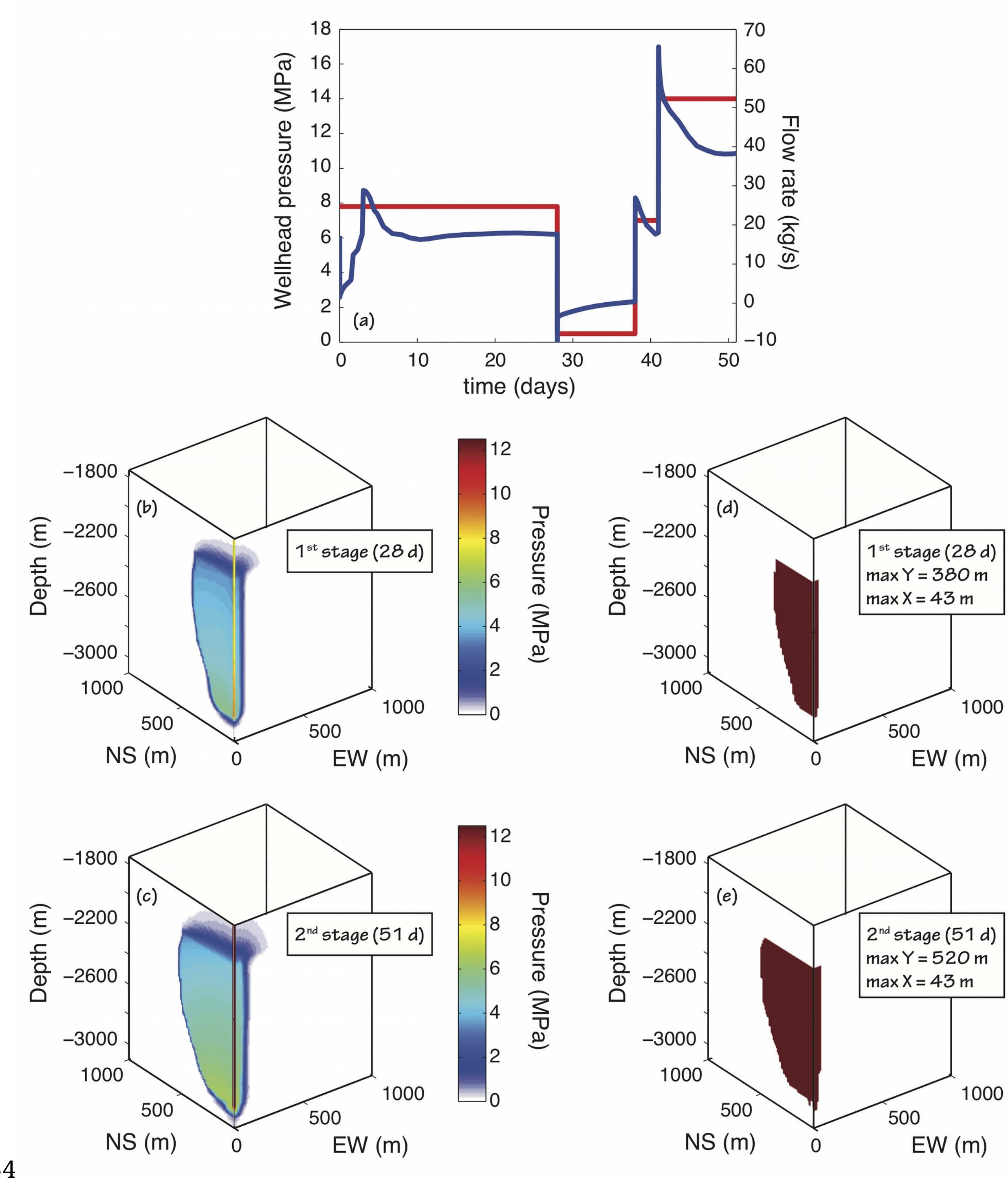

Figure 4. Simulation results for a system fully saturated with water. (a) Applied wellhead pressure (red) and resulting flow rate (blue). (b, c) Resulting pressure and hydrosheared zone at the end of the first stage (28 days). (d, e) Resulting pore pressure changes and hydrosheared zone at the end of the second stage (51 days).

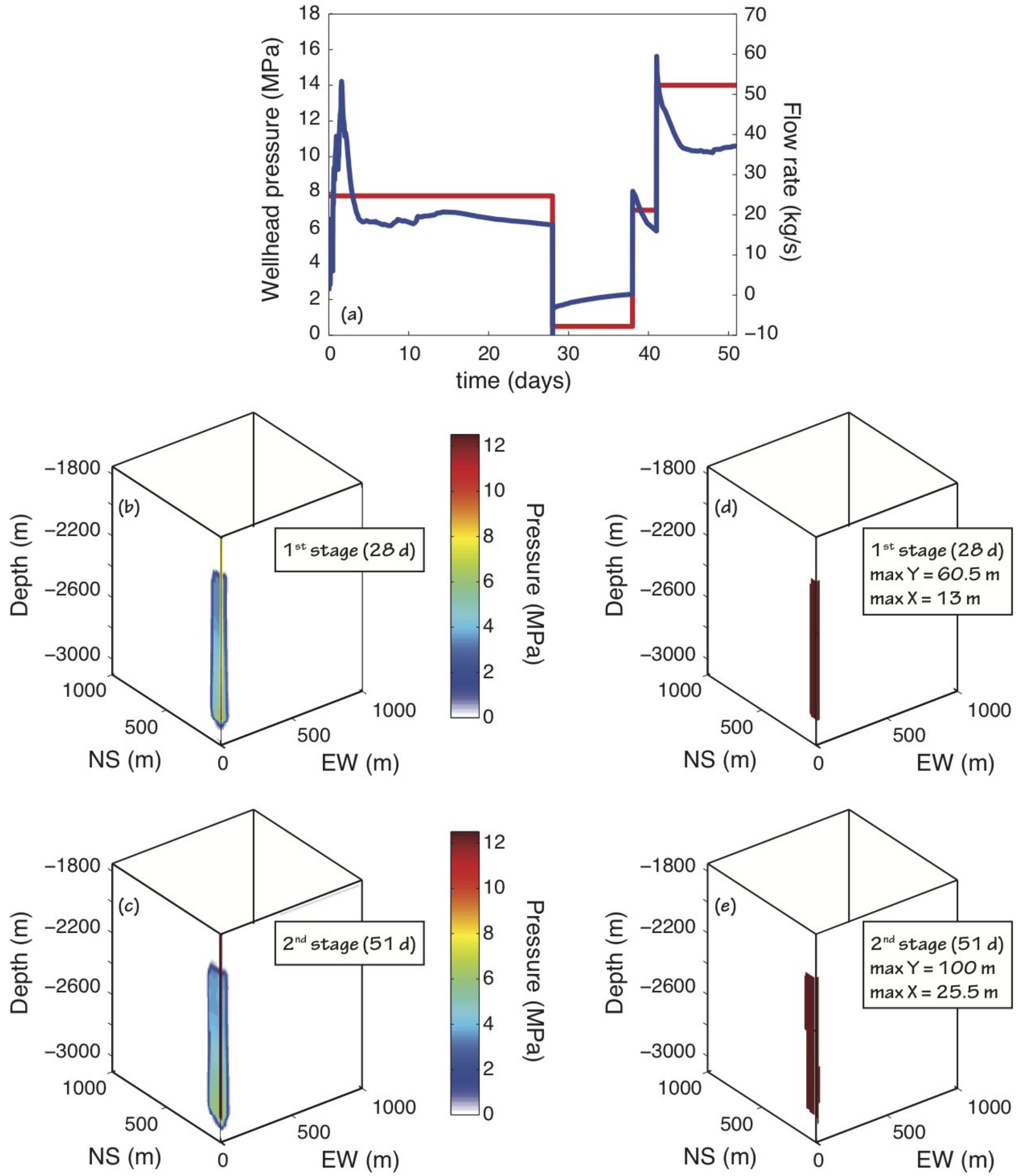

Figure 5. Simulation results for a system initially saturated with carbon dioxide. (a) Applied wellhead pressure (red) and resulting flow rate (blue). (b, c) Resulting pressure and hydrosheared zone at the end of the first stage (28 days). (d, e) Resulting pore pressure changes and hydrosheared zone at the end of the second stage (51 days).

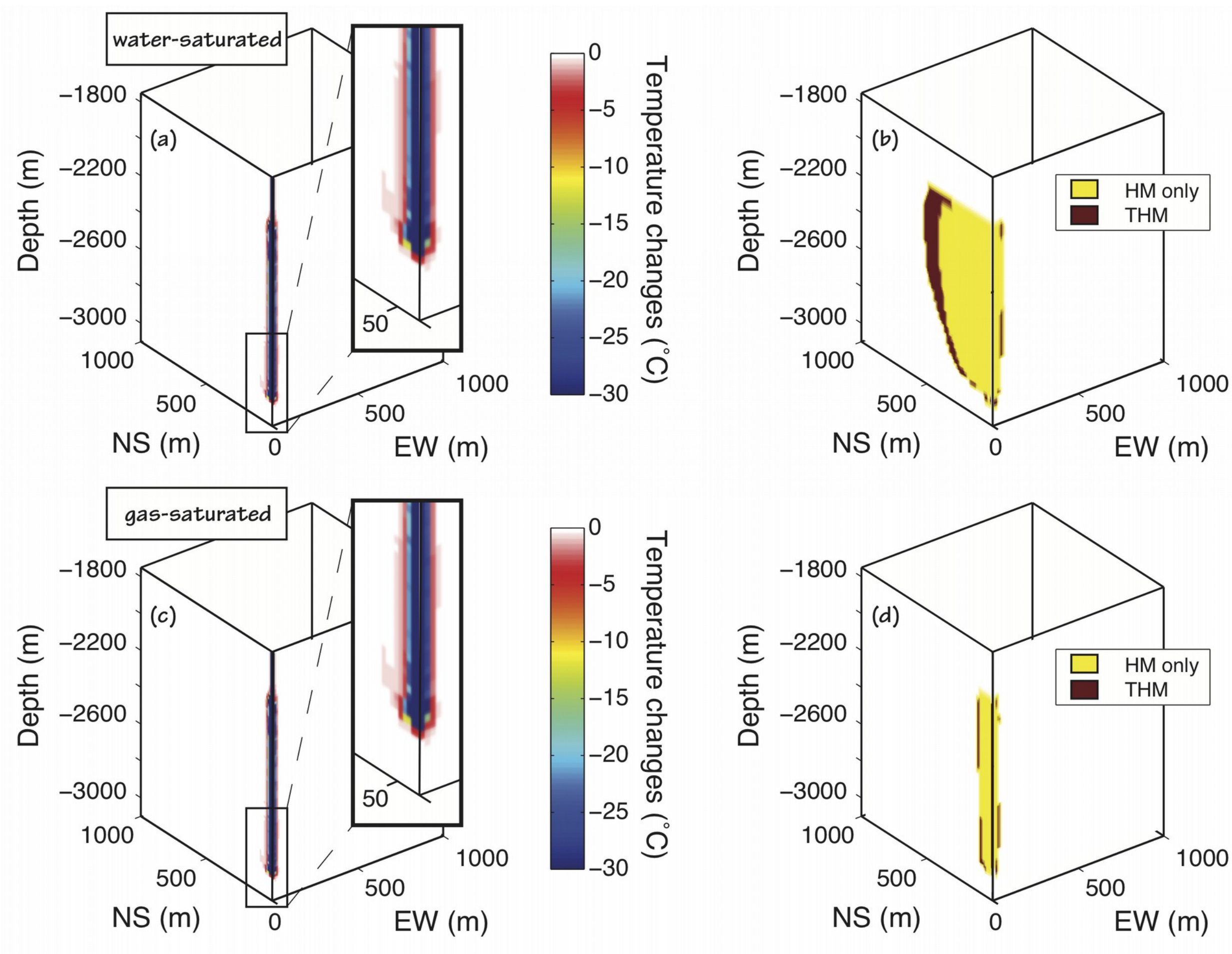

Figure 6. (a) Temperature changes after the stimulation and (b) resulting hydrosheared zone for THM (brown) and HM (yellow) modeling for a water-saturated system. (c) Temperature changes after the stimulation and (d) resulting hydrosheared zone for THM (brown) and HM (yellow) modeling for a system initially fully saturated with gas.

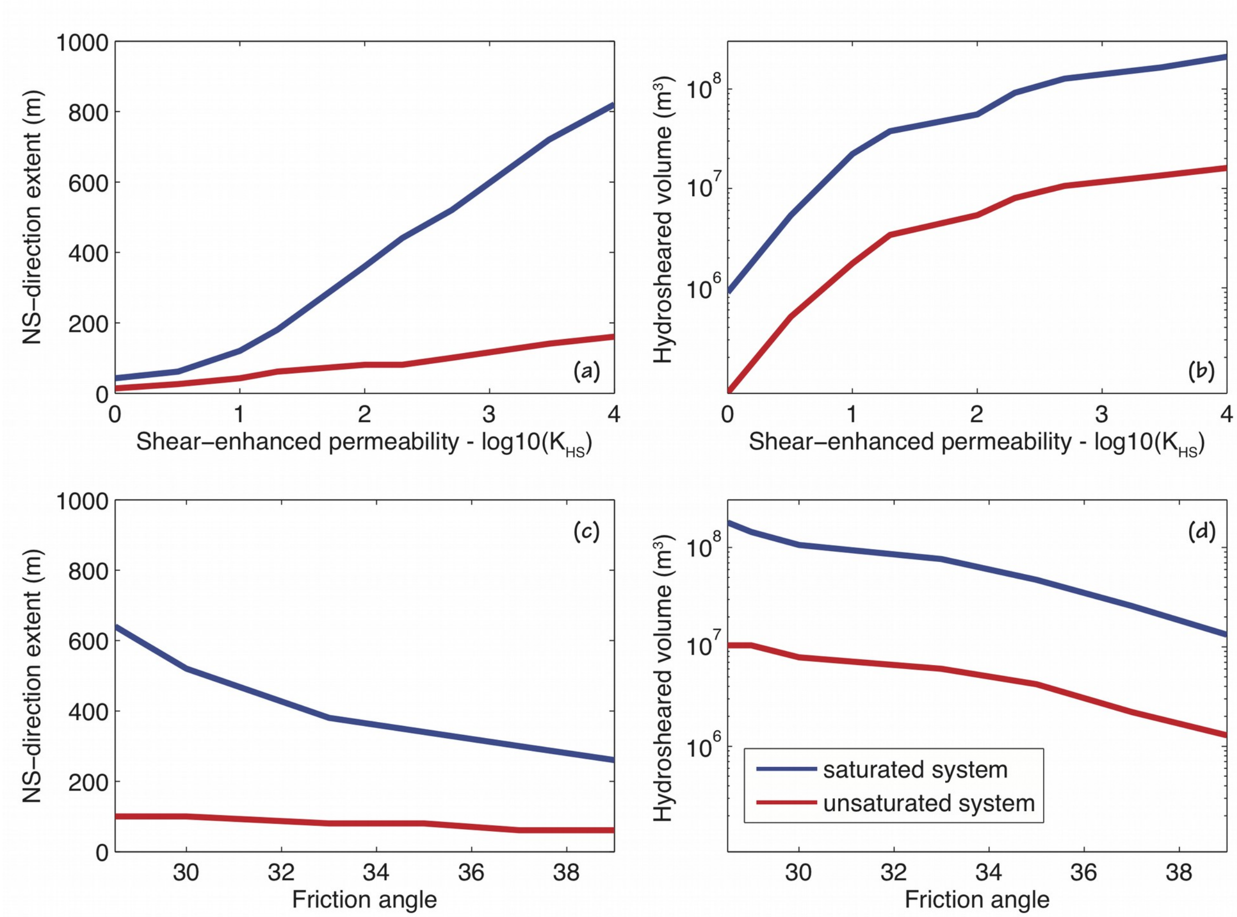

Figure 7. Sensitivity analysis. Blue and red lines refer to saturated and unsaturated systems, respectively. EGS reservoir extent along NS-direction (a) and hydrosheared volume (b) as a function of the constant for shear-enhanced permeability (K_{HS}, Eq. 6). EGS reservoir extent along NS-direction (c) and hydrosheared volume (d) as a function of the friction angle for the Mohr Coulomb criterion (□, Eq. 7).